Engineering Cellular Degradation of Multilayered Capsules through Controlled Cross-Linking

ARTICLE *in* ACS NANO · NOVEMBER 2012

Impact Factor: 12.88 · DOI: 10.1021/nn3039353 · Source: PubMed

Engineering Cellular Degradation of Multilayered Capsules through Controlled Cross-Linking

Kang Liang, Georgina K. Such, Zhiyuan Zhu, Sarah J. Dodds, Angus P. R. Johnston, Jiwei Cui, Hirotaka Ejima, and Frank Caruso*

Department of Chemical and Biomolecular Engineering, The University of Melbourne, Parkville, Victoria 3010, Australia

ABSTRACT We report a versatile approach for controlling the intracellular degradation of polymer capsules by tailoring the degree of cross-linking in the capsules. Poly(2-diisopropylaminoethyl methacrylate) capsules were assembled by the layer-by-layer technique and covalently stabilized with a redox-responsive bisazide cross-linker using click chemistry. The degree of cross-linking, determined using radiation scintillation counting, was tuned from 65% to 98% by adjusting the amount of cross-linker used to stabilize the polymer films. Transmission electron microscopy and fluorescence microscopy studies showed that the pH responsiveness of the capsules was maintained, regardless of the degree of cross-linking. Atomic force microscopy measurements on planar surfaces revealed that increasing the degree of cross-linking decreased the film roughness (from 8.7 to 1.7 nm), hence forming smoother films; however the film thicknesses were not significantly altered. Cellular studies showed that the rate of intracellular degradation of the capsules could be controlled between 0 and 6 h by altering the degree of cross-linking in the polymer capsules. These studies also demonstrated that the cellular degradation of highly cross-linked capsules (>90%) was significantly retarded compared to degradation in simulated cellular conditions. This suggests that the naturally occurring cellular reducing environment is rapidly depleted, and there is a significant delay before the cells can replenish the reducing environment. The modular and versatile nature of this approach lends itself to application to a wide range of polymer carriers and thus offers significant potential for the design of polymer-based systems for drug and gene delivery.

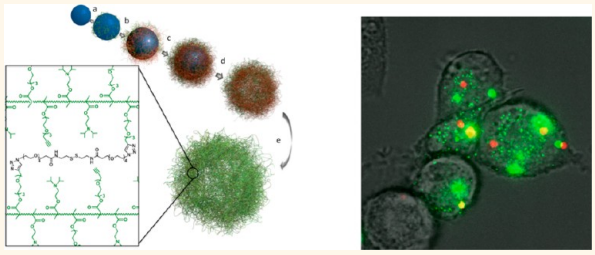

KEYWORDS: drug delivery · controlled degradation · controlled release · dual-responsive materials · layer-by-layer assembly · click chemistry

The design of polymer carriers with controlled degradation at a specific location (*e.g.*, subcellular compartments) is fundamental in drug/vaccine delivery and gene therapy applications.[1−5] Moreover, degradation of the carriers into smaller fragments enables them to be rapidly cleared from the body.[6] Recently, there has been significant interest in engineering carriers that exploit a biological trigger to induce their degradation and thus release encapsulated cargo.[7,8] Various mechanisms have been used to achieve targeted degradation in response to external triggers, including optical or magnetic stimulation, and changes in pH, enzymatic, and redox potentials.[8−15] pH- and redox-sensitive carriers have been widely investigated, as they are responsive to physiologically relevant conditions that naturally occur in cells. While there has been considerable research in this area,[16−19] most of these studies have focused on investigating their behavior in simulated biological conditions, which can be vastly different to their response in cells. There is limited work on tuning the degradation of drug carriers by specific biological triggers within cells. Control over degradation rate, and hence cargo release, is crucial for achieving efficient and effective delivery of a range of therapeutics.

Layer-by-layer (LbL) films, assembled by the sequential deposition of polymers through complementary interactions (*e.g.*, electrostatic, hydrogen bonding, covalent linkages) on particle templates,[4] are suitable candidates for controlled release applications. LbL assembly allows fine control over the film characteristics (*e.g.*, thickness, permeability, structure), assembly conditions, and subsequent processing steps for film stabilization and functionalization. Hydrogen-bonded LbL multilayers are of interest

* Address correspondence to fcaruso@unimelb.edu.au.

Received for review August 27, 2012 and accepted October 25, 2012.

Published online November 02, 2012
10.1021/nn3039353

because they can be designed to exhibit stimuli-responsive properties under physiologically relevant conditions; however, they have limited stability at physiological pH.[4] To overcome this, we developed a general approach for stabilizing these films by "clicking" hydrogen-bonded layers together with small molecule cross-linkers[20,21] through the copper-catalyzed azide−alkyne cycloaddition (CuAAC) reaction.[22] This approach provides rapid and specific assembly, and permits postfunctionalization in aqueous solutions under mild conditions.

We recently reported the LbL assembly of dual-responsive, alkyne-modified poly(2-diisopropylaminoethyl methacrylate) ($PDPA_{Alk}$) capsules that synergistically respond to pH and redox triggers.[23] PDPA-based materials are of significant interest as they are sensitive to physiological pH variations, therefore making them potentially useful for biomedical applications.[24,25] The $PDPA_{Alk}$ capsules were cross-linked by CuAAC using a bisazide cross-linker containing a central disulfide moiety. Disulfide groups are redox responsive, as they are stable in the bloodstream but cleavable in the presence of glutathione (GSH), which is an abundant intracellular thiol species.[26] These capsules rapidly degraded in simulated cellular conditions with only small amounts of GSH (0.01 to 1.5 mM). However, our previous study did not demonstrate control over the degradation rate of PDPA capsules,[23] which is often required for tuning the dosage of therapeutics and achieving multidrug release, and for controlling their behavior in cells.[27]

Herein, we report a simple and versatile technique for tuning the cellular degradation of LbL capsules. We have investigated the influence of the degree of cross-linking on PDPA films assembled on both planar and particle templates. Degradation of the capsules was studied under simulated cellular conditions and in cells using the JAWS II cell line. To our knowledge, this is the first report that demonstrates the tunable degradation of LbL capsules in cells. Importantly, significant differences were observed between degradation rates in simulated cellular conditions and in cells, particularly in the case of highly cross-linked (>90%) capsules. This has important implications for the design of redox-responsive delivery systems. The multilayer capsules were assembled through hydrogen bonding interactions between $PDPA_{Alk}$ and poly(methacrylic acid) (PMA) on silica particle templates at pH 4. To control degradation, the capsules were covalently stabilized with different molar quantities of a redox-responsive cross-linker to tune the degree of cross-linking. After template removal, PMA was expelled from the multilayer system by increasing the solution pH, which disrupts the hydrogen bonding between $PDPA_{Alk}$ and PMA, yielding single-component PDPA capsules with different degrees of cross-linking (Scheme 1). A radiolabeling method (scintillation counting of ^3H) was employed to quantitatively determine the number of

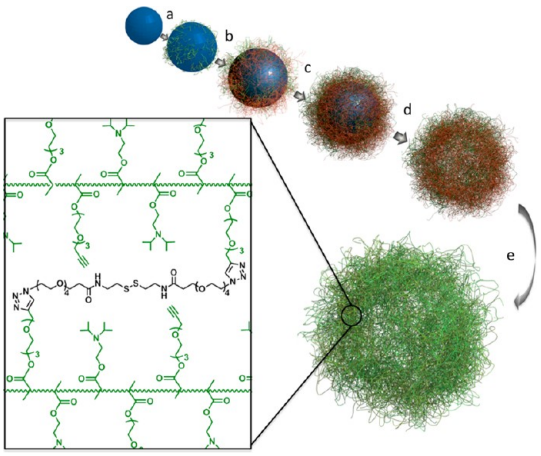

Scheme 1. Illustration of PDPA capsule assembly. (a−c) The multilayer films were assembled through LbL assembly between $PDPA_{Alk}$ and PMA on silica particle templates at pH 4. (d) After consecutive deposition of five $PDPA_{Alk}$/PMA bilayers, PDPA multilayers were covalently stabilized *via* click reactions between the alkyne moieties of PDPA and different amounts of bisazide cross-linker containing a disulfide bond in the presence of Cu(I), the particle template was dissolved, and (e) PMA layers were removed by raising the pH to 7.4, yielding single-component PDPA capsules with various degrees of cross-linking.

alkyne groups used in the cross-linking process and free alkyne groups in the capsules. Atomic force microscopy (AFM) measurements of hydrated planar films revealed differences in the surface topography (and roughness) as a result of different degrees of cross-linking. The degradation kinetics of the PDPA capsules were investigated using flow cytometry under simulated cellular conditions; and finally cellular uptake and degradation was assessed using the JAWS II cell line. Owing to the versatile nature of click systems, this tunable cross-linking technique could be extended to other systems to provide carriers with tailored properties for a range of drug delivery applications.

RESULTS AND DISCUSSION

$PDPA_{Alk}$/PMA multilayer films were first assembled on planar silicon substrates (1 cm^2) at pH 4 to examine changes in the physicochemical properties of the films that may relate to capsule morphologies and their degradation properties. A polyethyleneimine (PEI) prelayer and alkynated PMA (PMA_{Alk}) were deposited on the substrates prior to the $PDPA_{Alk}$/PMA layers to ensure the films remained anchored to the substrates after raising the pH. We have previously reported the homogeneous layer buildup between this polymer pair on both planar and silica particle surfaces.[23] After deposition of the five bilayers, a cross-linking solution containing copper(II) sulfate, sodium ascorbate, and bisazide linker was introduced to cross-link the $PDPA_{Alk}$ films. The amount of bisazide linker was systematically varied to tune the cross-linking degree of the films (Experimental Methods). The films were then washed with phosphate buffer (PBS) at pH 7.4. At pH < pK_a (6.4),

TABLE 1. AFM Analysis of PDPA Films Cross-Linked with Various Amounts of Cross-Linker; Measurements Carried out in pH 5.9 PBS

sample	amount of cross-linker, mol	concentration of cross-linker, M	film thickness[a], nm	RMS roughness, nm
A	5.0×10^{-13}	5.0×10^{-10}	20.1 ± 2.1	8.7 ± 0.3
B	5.0×10^{-12}	5.0×10^{-9}	22.8 ± 1.8	3.7 ± 0.2
C	1.3×10^{-11}	1.3×10^{-8}	23.9 ± 2.0	2.2 ± 0.1
D	2.5×10^{-11}	2.5×10^{-8}	23.8 ± 2.4	1.7 ± 0.1

[a] See also Supporting Information, Figure S2.

PDPA undergoes a charge-shifting transition from hydrophobic (water insoluble) to hydrophilic (water-soluble) due to protonation of its tertiary amine groups. Thus, when incubated in PBS the multilayers are destabilized, causing PMA to diffuse out of the $PDPA_{Alk}$ multilayers, leaving behind single-component, covalently stabilized PDPA films. Quartz crystal microbalance (QCM) measurements suggest that most of the PMA was removed from the PDPA multilayers upon changing the pH from 4 to 7.4 (Supporting Information, Figure S1).[23] Films were then transferred into pH 5.9 PBS to simulate endosomal pH conditions. AFM measurements were carried out on the hydrated films in PBS (Table 1 and Figure 1). The root-mean-square (RMS) roughness analysis (over $5 \times 5\ \mu m^2$) shows that, as the cross-linking concentration increases (Table 1 and Figure 1), the film morphology changes and the films become smoother (RMS from 8.7 to 1.7 nm). This indicates that the roughness of PDPA films can be tuned by simply varying the quantity of cross-linker added, without significantly affecting the total film thickness (see Table 1). The patchy topography of the least cross-linked film (Figure 1A) can be partly attributed to hydrophobic interactions of the PDPA causing the formation of domains. The weak cross-linking allows the PDPA to aggregate together to form these domains, whereas in the more highly cross-linked film (Figure 1D), the rigid film structure may not allow for film rearrangement to a similar degree. Furthermore, QCM measurements confirmed that after the removal of PMA the mass of cross-linked PDPA films was the same, irrespective of the amount of cross-linker added. However, 75% more non-cross-linked PDPA was removed from the 65% cross-linked film compared to the 98% cross-linked film when the films were transferred to pH 5.9, suggesting different film densities (Supporting Information, Figure S1).

To prepare PDPA capsules, $PDPA_{Alk}$ and PMA were sequentially deposited on 2.59 μm-diameter silica particles from 50 mM sodium acetate buffer (pH 4) and Milli Q water (pH 4), respectively. After the deposition of five bilayers, the same amount of cross-linker per unit surface area as the planar films was added to achieve the same degree of cross-linking (Supporting Information, Table S1). The silica templates were then removed using buffered hydrofluoric acid (HF). Free alkyne moieties that are not utilized in the cross-linking can be used for further functionalization, such as post-coupling of antibodies[28,29] and dyes for fluorescently labeling capsules.[20] The capsules were incubated in pH 7.4 PBS for 12 h to remove the PMA.

To determine the degree of cross-linking in these capsules, a radiolabeling method was employed. This allows the quantitative determination of free alkyne groups, rather than a qualitative measure, which is achieved using IR spectroscopy or fluorescence labeling. The capsules were cross-linked using four different reducible cross-linker amounts, ranging from 3.1×10^{-8} to 1.5×10^{-6} mol (Supporting Information, Table S1). Free accessible alkyne moieties remaining after the cross-linking step were reacted with tritiated, azide modified salicylic acid. Two assumptions were made in determining the degree of cross-linking: (1) Owing to the highly specific and reactive nature of the CuAAC reaction, and the relatively low molecular weight of the cross-linker (MW = 614.73), the cross-linker is expected to penetrate through the LbL layers and we assume that both sides of the bisazide linker can react with alkyne groups in the capsules. However, it is possible that some cross-linker will react with only one alkyne group, thus overestimating the degree of cross-linking. (2) The subsequent radiolabeling uses the same CuAAC reaction, and given that the radiolabeling molecule is small (MW = 179.13), we assume that the radiolabeling efficiency is close to 100%. A scintillation cocktail sensitive to β-emission was added and the radioactivity of each sample was then analyzed using liquid scintillation counting of ^3H (Figure 2). The difference in decay rate between the various cross-linked capsules and the non-cross-linked capsules accounts for the quantity of alkyne groups used in the cross-linking process. The removal of PMA and non-cross-linked $PDPA_{Alk}$ from the planar films was confirmed by QCM (Supporting Information, Figure S1). The total number of alkyne moieties in each capsule before cross-linking was calculated to be 2×10^5, ascertained from assessing the activity of non-cross-linked capsules. A systematic decrease in activity was observed with an increase in cross-linker concentration, indicating that more alkyne moieties were used in the cross-linking process (Supporting Information, Figure S3). This confirms the role of cross-linker concentration in controlling the degree of cross-linking in the capsules. It is noted that a certain cross-linking degree (>60%) is required to stabilize these PDPA capsules. From herein we denote the different amount of cross-linker added by the degree of

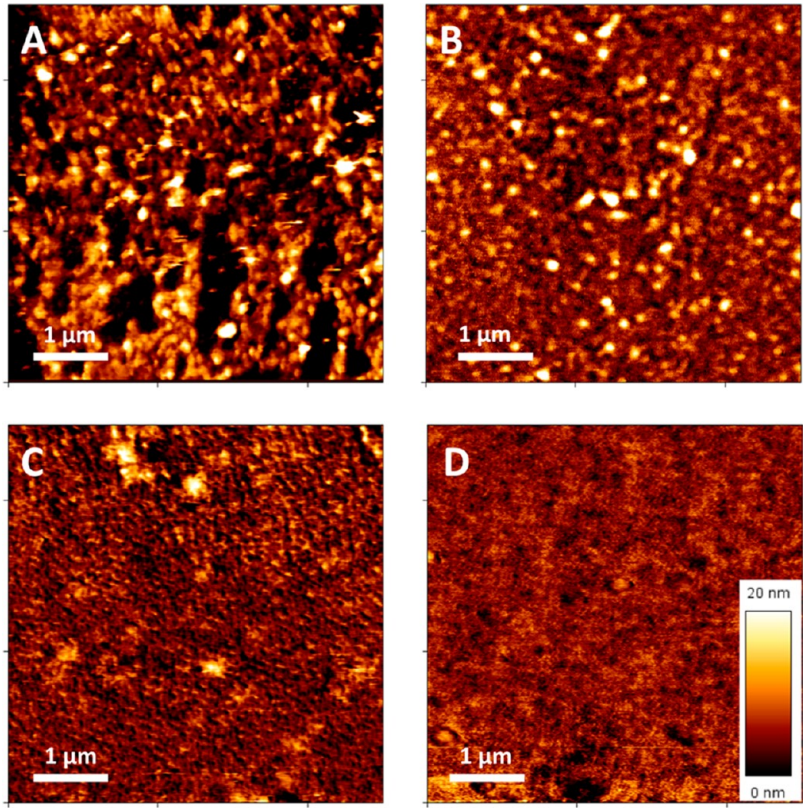

Figure 1. AFM images of PDPA films (5 layers) cross-linked with different quantities of bisazide cross-linker (see Table 1). Measurements were carried out in pH 5.9 PBS buffer. Height scales are the same for all of the images.

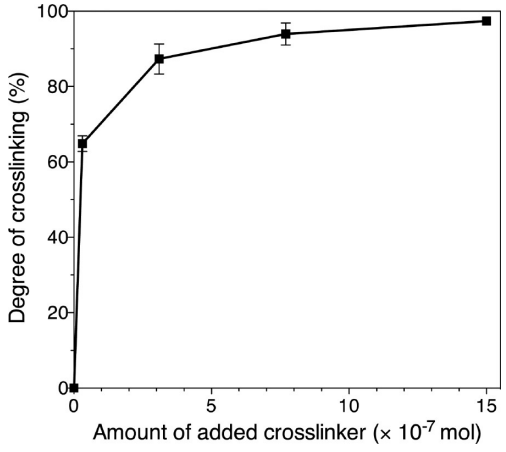

Figure 2. Degree of cross-linking of PDPA capsules as a function of added cross-linker. The degree of cross-linking was estimated on the basis of the total number of available alkyne groups in non-cross-linked capsules. Experiments were performed in duplicate.

cross-linking of the capsules. The degree of cross-linking of the capsules was 65% ($PDPA_{65\%}$), 87% ($PDPA_{87\%}$), 93% ($PDPA_{93\%}$), and 98% ($PDPA_{98\%}$) for bisazide cross-linker amounts of 3.1×10^{-8}, 3.1×10^{-7}, 7.7×10^{-7}, and 1.5×10^{-6} mol, respectively (Figure 2). It is noted that the cross-linking refers to the percentage of cross-linked alkyne groups and that the $PDPA_{Alk}$ used to assemble these capsules contained 10% alkyne groups.

The isolated capsules were analyzed using fluorescence microscopy and transmission electron microscopy (TEM). Despite the variation in cross-linking degree, capsules in all samples demonstrated similar responses to pH: the hydrophobic nature of PDPA at physiological pH provided the driving force for the shrinkage of the multilayers. A size reduction of approximately 50% was observed in all samples (Figure 3A), yet they remained colloidally stable. Upon reducing the pH, reswelling was observed (Figure 3B). The air-dried capsules on TEM copper grids showed folds and creases similar to a range of other polyelectrolyte capsules previously reported (Figure 3C, D; also see Supporting Information, Figure S4).[19−21,30]

This pH-responsiveness of PDPA capsules was designed to complement the physiological pH changes that occur during endocytosis. Under acidic conditions these capsules swell to twice their original diameter and the disulfide moieties become accessible, allowing degradation by intracellular thiol species,[23] which makes them promising for the delivery of drugs requiring intracellular release.[31,32] To examine whether the rate of degradation of PDPA capsules could be controlled by altering their degree of cross-linking, $PDPA_{65\%}$, $PDPA_{87\%}$, $PDPA_{93\%}$, and $PDPA_{98\%}$ capsules were degraded in simulated cellular conditions. As a control, nondegradable PDPA capsules cross-linked with a nonreducible bisazide cross-linker (equivalent to 87% cross-linking, Supporting Information, Figure S5) was

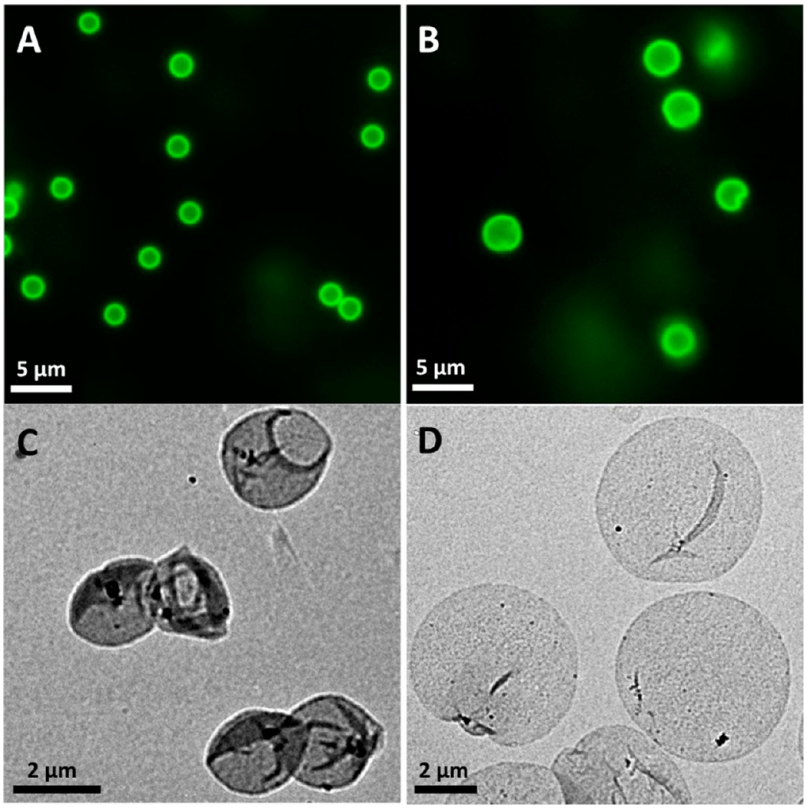

Figure 3. Representative fluorescence microscopy images of Alexa Fluor 488-labeled $PDPA_{87\%}$ capsules dispersed in (A) pH 7.4 PBS or (B) pH 5.9 PBS. TEM images of air-dried $PDPA_{87\%}$ capsules dispersed in (C) pH 7.4 PBS or (D) pH 5.9 PBS.

also used.[20] The capsules were then incubated at 37 °C in the presence of 0.5 mM GSH at pH 5.9 to simulate intracellular conditions. The exact intracellular concentration of the reducing species, such as GSH, is difficult to define and is highly dependent on both cell type and compartmentalization within cells. Several enzymes and proteins are important in regulating the GSH concentration in endosomes, and due to the dynamic influx and efflux of these enzymes across cellular compartments, the concentrations of these enzymes and proteins and hence GSH are difficult to determine.[33] Typically, total cellular GSH concentrations are quoted between 0.5 and 10 mM; however, often these concentrations are determined by lysing cells and thus the values quoted reflect an average, rather than a local concentration.[33−35] Therefore, we have chosen a low concentration (0.5 mM) to simulate the endosomal environment, as the concentration of reducing species within endosomes is likely to be lower than the cytoplasmic concentration. The total number of capsules in each sample was monitored over time by flow cytometry. A systematic decrease in degradation rate was observed with increasing cross-linking degree (from approximately 5 to 30 min to reach 50% of the capsule population, and approximately 20 to 90 min to reach 10% of the capsule population, Figure 4), highlighting the role of cross-linking degree in controlling the degradation profile of these capsules. In contrast, capsules cross-linked with the nonreducible linker showed no significant

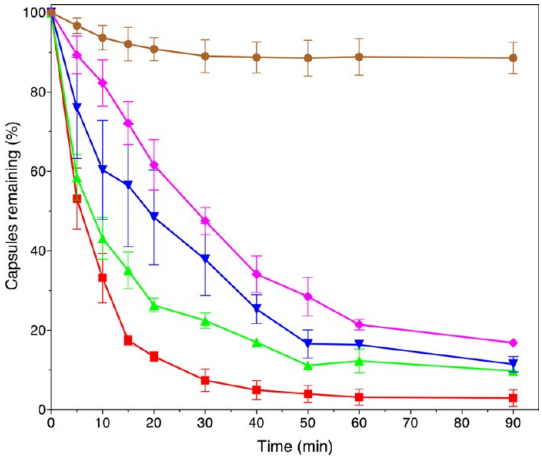

Figure 4. Degradation profiles of $PDPA_{65\%}$ (red squares), $PDPA_{87\%}$ (green triangles), $PDPA_{93\%}$ (blue triangles), and $PDPA_{98\%}$ (purple diamonds) capsules cross-linked with a bisazide redox-responsive linker, as monitored by flow cytometry. Control capsules were cross-linked at 87% (brown circles) using a nondegradable cross-linker. Experiments were performed in triplicate.

decrease in capsule numbers at the end of the assay (>90% remaining, Figure 4), suggesting these capsules remained stable. Furthermore, as previously reported, these capsules remained stable at pH 7.4, even with a 10-fold increase in GSH concentration (5 mM)[23].

Next, we examined the interaction between the $PDPA_{65\%}$, $PDPA_{87\%}$, $PDPA_{93\%}$, and $PDPA_{98\%}$ capsules

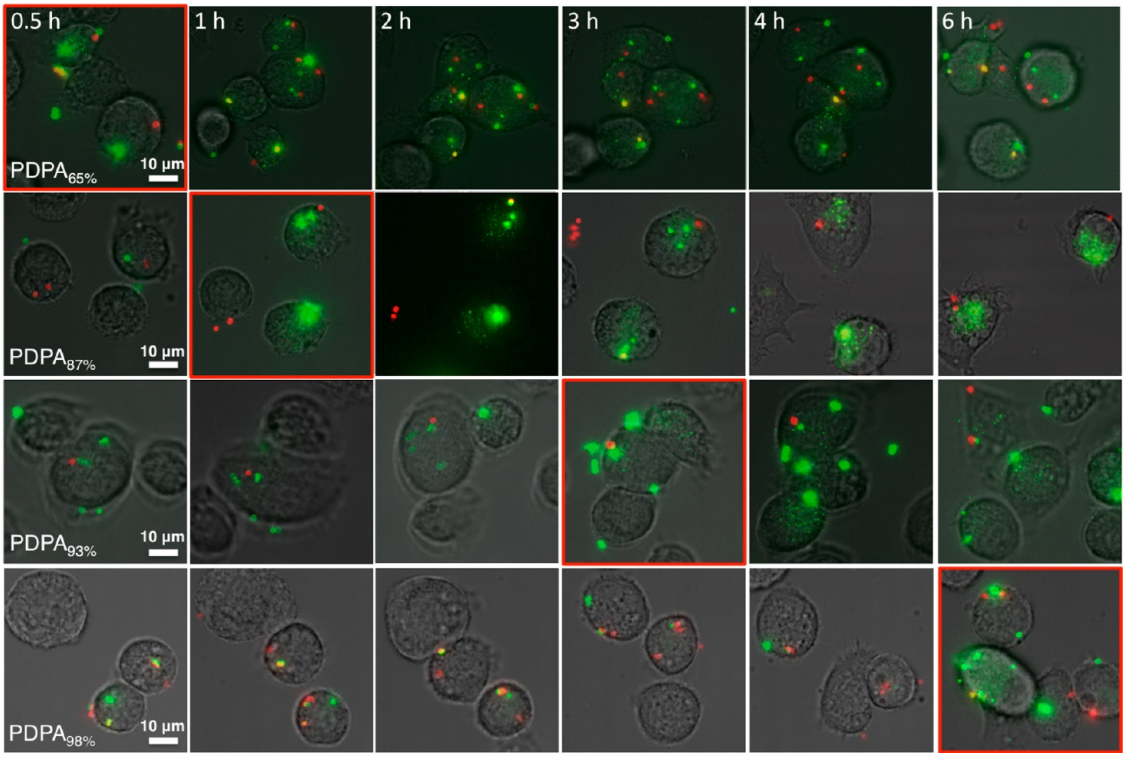

Figure 5. Deconvolution optical microscopy images (maximum intensity projection) of JAWS II cells incubated with degradable $PDPA_{65\%}$, $PDPA_{87\%}$, $PDPA_{93\%}$, and $PDPA_{98\%}$ capsules (green) cross-linked using a bisazide redox-responsive linker, or non-degradable PDPA capsules (red) (degree of cross-linking of 87%). Capsule/cell ratio of 20:1. Each row was focused on the same cells over time. Time frames that show the first evidence of capsule degradation are highlighted in red. Scale bars are the same for all images (see Supporting Information Figure S7 for enlarged images).

and JAWS II cells (at a capsule to cell ratio of approximately 20:1) as a function of time. Understanding the interactions between drug carriers and cells is one of the fundamental steps toward the delivery of therapeutics. JAWS II is an immortalized immature dendritic cell (DC) line, which was originally harvested from cultures of mouse bone marrow.[36] DCs are crucial for the activation of both T and B cells during an immune response *in vivo*,[37] and have therefore been widely studied for vaccination and immunotherapy against cancers and infectious diseases.[36] The cell association kinetics of the various cross-linked capsules with the cells at 37 °C was investigated using flow cytometry. The results showed a similar rate of cell association and uptake with time, irrespective of the amount of cross-linking (Supporting Information, Figure S6). This suggests that the cross-linking degree of PDPA capsules does not influence their cellular association with, or uptake by, JAWS II cells.

Degradable capsules were fluorescently labeled with Alexa Fluor 488 (nondegradable capsules were labeled with Alexa Fluor 647 as a control) and were incubated with JAWS II cells (at a capsule to cell ratio of approximately 20:1) at 4 °C for 4 h to associate the capsules with the cells but prevent cellular internalization. Unbound capsules were then rinsed off, and the temperature was raised to 37 °C to activate cellular uptake prior to live cell imaging. Figure 5 shows representative deconvolution optical microscopy images of cells incubated with capsules with different degrees of cross-linking at six time points. Each slice (*i.e.*, in the same *z*-plane) of a series of images was analyzed to verify if the capsule was outside or inside the cell membrane (Supporting Information, Figure S8). In all four samples (A–D), degradable capsules (green) were internalized, and degraded within the cells, as seen by the transformation over time of their shape from intact capsules to smaller fluorescent compartments. This pattern of fluorescence is indicative of fragmentation of the lysosomal compartment once the capsules have degraded within the lysosomes. Homogeneous fluorescence throughout the entire cell was not observed, suggesting that the degraded polymer remains compartmentalized, rather than being evenly distributed throughout the cell. We previously demonstrated that similar-sized LbL capsules are internalized into cancer cells *via* macropinocytosis, and localize within the lysosome.[38] In that work, while the capsules were cross-linked with degradable disulfide linkages, no fragmentation of the lysosomes was observed. This suggests that there was limited degradation of the capsules. In the current study, for fragmentation to occur, the structure of the capsule must be sufficiently degraded so that free polymer, or fragments of polymer, are able to bud off into different compartments. In contrast to the redox-responsive capsules, capsules cross-linked with the non-degradable linker (red) remained intact, suggesting no

significant degradation in the cells. Selective intracellular degradation can therefore be readily achieved through variation of the cross-linker for stabilizing the multilayered capsules.

$PDPA_{65\%}$ capsules showed significant degradation at the start of the experiment (less than 30 min). In comparison, $PDPA_{98\%}$ capsules showed no significant degradation until 6 h after the capsules were internalized by the cells. Control of the degradation rate within the cells was achieved by varying the degree of cross-linking in the capsules. Increasing the degree of cross-linking from 65% to 87% delayed the onset of degradation and fragmentation by approximately 60 min. Further increasing the degree to 93% delayed the signs of degradation for approximately 3 h (Figure 5). This emphasizes the role of the degree of cross-linking in controlling the intracellular degradation rate.

Furthermore, by comparing these results to degradation profiles measured in simulated conditions (Figure 4), different degradation kinetics were observed. The capsules with a low degree of cross-linking (67%) degraded within 30 min in both conditions. However, for capsules with higher degrees of cross-linking, a significantly delayed degradation response was observed in the cells compared to simulated conditions (1 h in cells for 87% cross-linking, compared to 30 min in simulated conditions, and 6 h in cells for 98% cross-linking compared to 90 min in simulated conditions, see Supporting Information, Figure S7). This suggests that the GSH concentration within the endosome is depleted as the cells degrade the capsules. We speculate that once the GSH is consumed, there is a significant delay before the cell can synthesize fresh GSH and it can diffuse into the endosomal compartments. This results in the cells being able to effectively process PDPA capsules with less cross-linking (<90%); however, highly cross-linked capsules (>90%) are processed more slowly. These capsules demonstrate increased cellular response over disulfide-cross-linked PMA (PMA_{SH}) capsules that we have previously reported, but no significant degradation within the cells was observed using TEM.[38] This is due to the greater number of disulfide linkages in PMA_{SH} capsules and/or the use of PMA, which undergoes shrinkage at endosomal pH, thus making the PMA_{SH} capsules less sensitive to changes in redox-potential compared with the PDPA capsules. This delayed cellular response highlights the complexity that exists in the cells compared to simulated cellular conditions, and also suggests that it is important to consider the amount of disulfide groups used when designing new therapeutic delivery vehicles. Moreover, the cells remained healthy throughout the experiments (Figure 5), indicating that PDPA capsules have negligible impact on cell viability, which is also in agreement with the MTT assay reported previously.[23] We have previously demonstrated the loading and release of a model antigen (OVA) from these capsules,[23] and the control over capsule degradation demonstrated in the current work is expected to improve the efficiency of drug and antigen delivery.[39]

CONCLUSIONS

In summary, we have presented a versatile approach to control the degradation profile of polymeric capsules, in both stimulated cellular conditions and in cells, by varying the degree of cross-linking, which was achieved by adjusting the quantity of cross-linker used to stabilize the polymer films. Using this approach, the roughness of the films on planar supports could be finely tuned without affecting the thickness of the film. The resultant PDPA capsules showed similar reversible size changes with pH. The onset of degradation of capsules in JAWS II cells was controlled from being almost instantaneous for 65% cross-linking, to being delayed by 6 h for 98% cross-linking. The cellular degradation differed significantly from the degradation in simulated cellular conditions. This highlights the significance of cross-linking degree in controlling the cellular responses. The controlled degradation of PDPA capsules holds promise for intracellular delivery of therapeutics, DNA, protein, and vaccines, which often require specific release rates to enhance their therapeutic outcomes.

EXPERIMENTAL METHODS

Materials. Sodium acetate anhydrous, phosphate buffered saline (PBS), and reduced L-glutathione (GSH) were purchased from Sigma–Aldrich. 2-Diisopropylaminoethylmethacrylate (DPA) and poly(methacrylic acid) (PMA, 15 kDa) were obtained from Polysciences (USA). Nonporous colloidal SiO_2 particles (2.59 μm average diameter) were obtained from Microparticles GmbH (Berlin, Germany). Alexa Fluor 488 azide, and Alexa Fluor 647 azide (triethylammonium salt) were purchased from Invitrogen. Tritiated 4-azidosalicylic acid [ring-5-3H] (1 mCi/mL in ethanol) was purchased from American Radiolabeled Chemicals, and ultima Gold scintillation cocktail was obtained from PerkinElmer. All other materials were obtained from Sigma–Aldrich and used as received.

High purity and resistivity (18.2 M Ω cm) deionized water (Milli Q) was obtained from an inline Millipore RiOs/origin water purification system. Silicon wafers were obtained from MMRC Pty Ltd. (Melbourne, Australia). Cleaning of silicon wafers for AFM experiments was performed by submerging slides in Piranha solution (70/30 v/v sulfuric acid/hydrogen peroxide) for 10 min and rinsing thoroughly with water. [*Caution! Piranha solution is highly corrosive. Extreme care should be taken when handling Piranha solution and only small quantities should be prepared.*] The slides were then sonicated in 50 v/v isopropyl alcohol/water for 15 min. Following this, the slides were heated to 60 °C in RCA solution (5:1:1 water/hydrogen peroxide/ammonia solution) for 20 min. Finally, substrates were washed with water and dried under a stream of nitrogen.

Polymer and Linker Synthesis. Details of the synthesis of PDPA with alkyne moieties (referred to as $PDPA_{Alk}$) can be found in our previous publication.[23] Details of the synthesis of the nonreducible cross-linker (bisazido dodecaethylene glycol)

and the disulfide-containing bisazide linker can be found elsewhere.[20,21]

Multilayer Assembly on Planar Supports. For ($PDPA_{Alk}$/PMA) multilayer assembly, polyethylenimine- and PMA_{Alk}-coated silicon wafer slides (1 cm^2) were sequentially immersed into sodium acetate buffer solutions (pH 4, 50 mM) containing 1 mg mL^{-1} of $PDPA_{Alk}$ or PMA in Milli Q water (pH 4). A period of 15 min was allowed for the deposition of each layer, followed by immersion in acetate buffer for 1 min three times. After deposition of five consecutive bilayers, the multilayers were cross-linked by incubation in solutions containing various amounts of the bisazide cross-linker, sodium ascorbate (4.4 mg mL^{-1}), and copper sulfate (1.8 mg mL^{-1}) at pH 4 for 24 h. The final volume in each sample was 1 mL. Removal of PMA from cross-linked PDPA multilayers was achieved by incubation in PBS (pH 7.4) overnight, followed by three PBS (pH 7.4) washings for 1 min. The silicon wafers were then reimmersed into PBS (pH 6) before AFM analysis in liquid.

Capsule Preparation. A 100 μL aliquot of a SiO_2 particle suspension (5 wt %, 2.59 μm average diameter) was centrifuged and washed three times in sodium acetate buffer (pH 4, 50 mM). This procedure was used as the standard washing procedure. Assembly of the polymers was achieved by consecutive incubation of the silica templates with 200 μL of PMA (1 mg mL^{-1}) at pH 4 and 200 μL of alkyne-functionalized poly-(2-(diisopropylamino)ethyl methacrylate) ($PDPA_{Alk}$, 12 kDa, 1 mg mL^{-1}) at pH 4 in 50 mM sodium acetate buffer with constant shaking at 23 °C. A 15 min adsorption time was allowed for all layers, and particles underwent three centrifugation/wash cycles before the addition of the following layer. This procedure was repeated until five bilayers of $PDPA_{Alk}$/PMA were adsorbed. The multilayers were then cross-linked by incubation in solutions containing various amounts of the bisazide cross-linker, sodium ascorbate (4.4 mg mL^{-1}), and copper sulfate (1.8 mg mL^{-1}) at pH 4 for 24 h with constant shaking. Removal of the SiO_2 particles to form hollow capsules was achieved by mixing the particle suspension with ammonium fluoride (13.3 M) buffered HF (5 M) at a volumetric ratio of 1:1.5. The capsules were then washed three times through centrifugation/wash cycles in pH 4, 50 mM sodium acetate buffer. The removal of electrostatically bound PMA layers from the cross-linked PDPA multilayers was achieved by incubating capsules in PBS overnight followed by three centrifugation/wash cycles in PBS.

Determination of the Degree of Capsule Cross-Linking. PDPA capsule samples (prepared on 2.59 μm diameter silica templates, 2×10^8 capsules/sample) cross-linked to different degrees with the bisazide cross-linker were prepared in duplicate and suspended in 200 μL of sodium acetate buffer (50 mM, pH 4). One sample from each pair was incubated with 10 μL of tritiated 4-azidosalicylic acid (500 μCi mL^{-1}) in the presence of 50 μL of copper sulfate (1.8 mg mL^{-1} in 50 mM sodium acetate) and 50 μL of sodium ascorbate (4.4 mg mL^{-1} in 50 mM sodium acetate) for 2 h with regular agitation. The remaining sample from each pair (no copper catalyst control) was incubated with 10 μL of tritiated 4-azidosalicylic acid (500 μCi mL^{-1}) in the presence of 100 μL of 50 mM sodium acetate buffer (pH 4) and otherwise treated the same as the catalyzed samples. After incubation, samples were isolated by centrifugation and 200 μL was collected from the supernatant. A 200 μL aliquot of sodium acetate buffer (50 mM, pH 4) was added, and the centrifugation and supernatant removal was repeated. This washing step was completed a further four times. After the final washing step 270 μL of DTT (50 mM in 50 mM sodium acetate buffer) was added to each sample in the presence of 30 μL of hydrochloric acid (1 M). The non-cross-linked sample (0 M cross-linker) was treated with 300 μL of sodium hydroxide (0.5 M). Samples of the wash supernatants and 10% of each degraded capsule sample were added to 5 mL scintillation vials, Ultima Gold scintillation cocktail (2 mL) was added, and the samples were well mixed. Activity was measured using a PerkinElmer Tri-Carb 2800TR Liquid Scintillation Analyzer.

Fluorescent Labeling of Capsules. For a starting volume of 100 μL particles, 1.5 μL of Alexa Fluor 488 azide or Alexa Fluor 647 azide (1 mg mL^{-1} in DMSO), 50 μL of sodium ascorbate (4.4 mg mL^{-1}), and 50 μL of copper sulfate (1.8 mg mL^{-1}) were added in 150 μL of sodium acetate buffer (pH 4, 50 mM) to the cross-linked particles with constant shaking overnight. The particles were washed three times before the removal of core templates.

Degradation of $PDPA_{Alk}$ Capsules. Cross-linked and fluorescently labeled PDPA capsules were washed into PBS and counted using flow cytometry. Then, a set of samples with a total capsule population of 1×10^7 was prepared by mixing with glutathione (GSH, 0.5 mM) in PBS buffer, the pH of which was adjusted to 6. The samples were incubated at 37 °C with constant shaking at 500*g*. At each measurement, approximately 5×10^4 capsules were assessed. The mean fluorescence intensity and the number of capsules were measured to determine the degradation of capsules that resulted from capsule swelling due to pH, and from capsule degradation *via* GSH reduction of the cross-linker.

Live Cell Imaging. JAWS II cells were seeded in an 8-well chambered cover glass (Thermo Scientific) at 37 °C (5% CO_2) overnight at a population of 50 000 cells per well. The cells were then incubated at 4 °C. Capsules cross-linked with different amounts of cross-linker were added at a capsule/cell ratio of 20:1 in each well. Nondegradable capsules were also added at the same ratio as a control. After 4 h, the cells were washed with warm media (37 °C) twice to remove free-floating capsules. The cells were finally covered with 500 μL of media in each well. The cover glass was then fitted in a DeltaVision (Applied Precision) microscope. Cells were kept alive in the incubation chamber, equipped with a CO_2 inlet, at 37 °C and mounted on the microscope stage, for imaging. Live cell imaging was performed for 12 h on five random spots chosen in each well. Each experiment was performed in triplicate. Deconvolution images were taken on a series of *z*-sections within the top and bottom of the cells at a time lapse of 30 min for 12 h. Each slice of the images (*i.e.*, in the same *z*-plane) was analyzed to verify if the capsule was either on the outside or inside of the cell membrane.

Capsule-Cell Association Kinetics. JAWS II cells were seeded in a 24-well plate at 37 °C (5% CO_2) overnight at a population of 40 000 cells per well. The cells were then incubated at 4 °C. Capsules cross-linked with different amounts of cross-linker were added at a capsule/cell ratio of 20:1 in each well. Nondegradable capsules were also added at the same ratio as a control. At each time point, the cells were washed with warm media (37 °C) twice to remove free-floating capsules. One mL of 1× trypsin was added to lift the cells. The cells were then centrifuged and washed twice to remove trypsin before being transferred to flow cytometry tubes. This experiment was carried out in triplicate.

Analytical Methods. For AFM measurements in liquid, samples prepared on silica wafers were mounted on a NanoWizard II AFM (JPK Instruments, Berlin, Germany) in intermittent contact in liquid mode with Veeco silicon nitride cantilevers (MLCT). Samples were immersed in pH 5.9 PBS buffer at 37 °C while conducting the measurements. Film roughness and thickness were analyzed using JPK SPM Image Processing software (V.3.3.32). TEM images were taken with a Philips CM120 BioTWIN TEM at an operation voltage of 120 kV. Samples of capsules were air-dried on a carbon-coated Formvar film mounted on 300 mesh copper grids (ProSciTech, Australia). Fluorescence images were taken on an inverted Olympus IX71 microscope equipped with a 60× objective lens (Olympus UPFL20/0.5 NA, W.D. 1.6). A CCD camera was mounted on the left-hand port of the microscope. Fluorescence images were illuminated with an X-Cite module. Deconvolution fluorescence microscopy was performed on a DeltaVision (Applied Precision) microscope with a 60× 1.42 NA oil objective with a standard FITC/TRITC/CY5 filter set. Images were processed with Imaris (Bitplane) using the maximum intensity projection. Flow cytometry measurements were carried out on a Partec CyFlow Space (Partec GmbH, Germany) flow cytometer at an excitation wavelength of 488 and 647 nm. Each experiment was performed in triplicate. Analysis was performed using FlowJo v8.7 (TreeStar).

Conflict of Interest: The authors declare no competing financial interest.

Acknowledgment. This work was supported by the Australian Research Council under the Federation Fellowship (F.C.), Future Fellowship (A.P.R.J), and Discovery Project (F.C., A.P.R.J., and G.K.S.) schemes.

Supporting Information Available: Cross-linker amounts and concentrations added in each silica particle suspension, AFM thickness analysis of PDPA films, structure of the nonreducible bisazide cross-linker, available alkyne groups in each capsule after different degrees of cross-linking, pH responsiveness analysis of PDPA capsules, capsule-cell association kinetics, and enlarged microscopy images of cells incubated with PDPA capsules with different degrees of cross-linking. This material is available free of charge *via* the Internet at http://pubs.acs.org.

REFERENCES AND NOTES

1. Duncan, R. The Dawning Era of Polymer Therapeutics. *Nat. Rev. Drug Discovery* **2003**, *2*, 347–360.
2. Dobrovolskaia, M. A.; McNeil, S. E. Immunological Properties of Engineered Nanomaterials. *Nat. Nanotechnol.* **2007**, *2*, 469–478.
3. LaVan, D. A.; Lynn, D. M.; Langer, R. Moving Smaller in Drug Discovery and Delivery. *Nat. Rev. Drug Discovery* **2002**, *1*, 77–84.
4. Such, G. K.; Johnston, A. P. R.; Caruso, F. Engineered Hydrogen-Bonded Polymer Multilayers: From Assembly to Biomedical Applications. *Chem. Soc. Rev.* **2011**, *40*, 19–29.
5. Johnston, A. P. R.; Lee, L.; Wang, Y.; Caruso, F. Controlled Degradation of DNA Capsules with Engineered Restriction-Enzyme Cut Sites. *Small* **2009**, *5*, 1418–1421.
6. Owens, D. E., III; Peppas, N. A. Opsonization, Biodistribution, and Pharmacokinetics of Polymeric Nanoparticles. *Int. J. Pharm.* **2006**, *307*, 93–102.
7. Johnston, A. P. R.; Such, G. K.; Caruso, F. Triggering Release of Encapsulated Cargo. *Angew. Chem., Int. Ed.* **2010**, *49*, 2664–2666.
8. De Geest, B. G.; Sanders, N. N.; Sukhorukov, G. B.; Demeester, J.; De Smedt, S. C. Release Mechanisms for Polyelectrolyte Capsules. *Chem. Soc. Rev.* **2006**, *36*, 636–649.
9. Tong, R.; Christian, D. A.; Tang, L.; Cabral, H.; Baker, J. R.; Kataoka, K.; Discher, D. E.; Cheng, J. Nanopolymeric Therapeutics. *MRS Bull.* **2009**, *34*, 422–431.
10. Delcea, M.; Möhwald, H.; Skirtach, A. G. Stimuli-Responsive LbL Capsules and Nanoshells for Drug Delivery. *Adv. Drug Delivery Rev.* **2011**, *63*, 730–747.
11. Nishiyama, N.; Kataoka, K. Current State, Achievements, and Future Prospects of Polymeric Micelles as Nanocarriers for Drug and Gene Delivery. *Pharmacol. Ther.* **2006**, *112*, 630–648.
12. Kim, K. T.; Meeuwissen, S. A.; Nolte, R. J. M.; van Hest, J. C. M. Smart Nanocontainers and Nanoreactors. *Nanoscale* **2010**, *2*, 844–858.
13. De Geest, B. G.; Vandenbroucke, R. E.; Guenther, A. M.; Sukhorukov, G. B.; Hennink, W. E.; Sanders, N. N.; Demeester, J.; De Smedt, S. C. Intracellularly Degradable Polyelectrolyte Microcapsules. *Adv. Mater.* **2006**, *18*, 1005–1009.
14. De Koker, S.; De Geest, B. G.; Singh, S. K.; De Rycke, R.; Naessens, T.; Van Kooyk, Y.; Demeester, J.; De Smedt, S. C.; Grooten, J. Polyelectrolyte Microcapsules as Antigen Delivery Vehicles to Dendritic Cells: Uptake, Processing, and Cross-Presentation of Encapsulated Antigens. *Angew. Chem., Int. Ed.* **2009**, *48*, 8485–8489.
15. Rivera-Gil, P.; De Koker, S.; De Geest, B. G.; Parak, W. J. Intracellular Processing of Proteins Mediated by Biodegradable Polyelectrolyte Capsules. *Nano Lett.* **2009**, *9*, 4398–4402.
16. Duan, H.; Kuang, M.; Zhang, G.; Wang, D.; Kurth, D. G.; Möhwald, H. pH-Responsive Capsules Derived from Nanocrystal Templating. *Langmuir* **2005**, *21*, 11495–11499.
17. Zhao, M.; Biswas, A.; Hu, B.; Joo, K.-I.; Wang, P.; Gu, Z.; Tang, Y. Redox-Responsive Nanocapsules for Intracellular Protein Delivery. *Biomaterials* **2011**, *32*, 5223–5230.
18. Ma, Y.; Dong, W.; Hempenius, M. A.; Möhwald, H.; Vancso, G. J. Redox-Controlled Molecular Permeability of Composite-Wall Microcapsules. *Nat. Mater.* **2006**, *5*, 724–729.
19. Leung, M. K. M.; Such, G. K.; Johnston, A. P. R.; Biswas, D. P.; Zhu, Z.; Yan, Y.; Lutz, J. F.; Caruso, F. Assembly and Degradation of Low-Fouling Click-Functionalized Poly(ethylene glycol)-Based Multilayer Films and Capsules. *Small* **2011**, *7*, 1075–1085.
20. Kinnane, C. R.; Such, G. K.; Antequera-García, G.; Yan, Y.; Dodds, S. J.; Liz-Marzan, L. M.; Caruso, F. Low-Fouling Poly(*N*-vinyl pyrrolidone) Capsules with Engineered Degradable Properties. *Biomacromolecules* **2009**, *10*, 2839–2846.
21. Ochs, C. J.; Such, G. K.; Yan, Y.; van Koeverden, M. P.; Caruso, F. Biodegradable Click Capsules with Engineered Drug-Loaded Multilayers. *ACS Nano* **2010**, *4*, 1653–1663.
22. Such, G. K.; Tjipto, E.; Postma, A.; Johnston, A. P. R.; Caruso, F. Ultrathin, Responsive Polymer Click Capsules. *Nano Lett.* **2007**, *7*, 1706–1710.
23. Liang, K.; Such, G. K.; Zhu, Z.; Yan, Y.; Lomas, H.; Caruso, F. Charge-Shifting Click Capsules with Dual-Responsive Cargo Release Mechanisms. *Adv. Mater.* **2011**, *23*, H273–H277.
24. Du, J.; Tang, Y.; Lewis, A. L.; Armes, S. P. pH-Sensitive Vesicles Based on a Biocompatible Zwitterionic Diblock Copolymer. *J. Am. Chem. Soc.* **2005**, *127*, 17982–17983.
25. Lomas, H.; Johnston, A. P. R.; Such, G. K.; Zhu, Z.; Liang, K.; van Koeverden, M. P.; Alongkornchotikul, S.; Caruso, F. Polymersome-Loaded Capsules for Controlled Release of DNA. *Small* **2011**, *7*, 2109–2119.
26. Meister, A.; Anderson, M. E. Glutathione. *Annu. Rev. Biochem.* **1983**, *52*, 711–760.
27. Loretta, L.; Rivera-Gil, P.; Abbasi, A. Z.; Ochs, M.; Ganas, C.; Zins, I.; Sonnichsen, C.; Parak, W. J. LbL Multilayer Capsules: Recent Progress and Future Outlook for Their Use in Life Sciences. *Nanoscale* **2010**, *2*, 458–467.
28. Kamphuis, M. M. J.; Johnston, A. P. R.; Such, G. K.; Dam, H. H.; Evans, R. A.; Scott, A. M.; Nice, E. C.; Heath, J. K.; Caruso, F. Targeting of Cancer Cells Using Click-Functionalized Polymer Capsules. *J. Am. Chem. Soc.* **2010**, *132*, 15881–15883.
29. Johnston, A. P. R.; Kamphuis, M. M. J.; Such, G. K.; Scott, A. M.; Nice, E. C.; Heath, J. K.; Caruso, F. Targeting Cancer Cells: Controlling the Binding and Internalization of Antibody-Functionalized Capsules. *ACS Nano* **2012**, *6*, 6667–6674.
30. Gao, C.; Leporatti, S.; Moya, S.; Donath, E.; Möhwald, H. Stability and Mechanical Properties of Polyelectrolyte Capsules Obtained by Stepwise Assembly of Poly(styrenesulfonate sodium salt) and Poly(diallyldimethyl ammonium) Chloride onto Melamine Resin Particles. *Langmuir* **2001**, *17*, 3491–3495.
31. Li, C. Poly(-glutamic acid)-Anticancer Drug Conjugates. *Adv. Drug Delivery Rev.* **2002**, *54*, 695–713.
32. Wang, Y.; Yan, Y.; Cui, J.; Hosta-Rigau, L.; Heath, J. K.; Nice, E. C.; Caruso, F. Encapsulation of Water-Insoluble Drugs in Polymer Capsules Prepared Using Mesoporous Silica Templates for Intracellular Drug Delivery. *Adv. Mater.* **2010**, *22*, 4293–4297.
33. Bauhuber, S.; Hozsa, C.; Breunig, M.; Göpferich, A. Delivery of Nucleic Acids *via* Disulfide-Based Carrier Systems. *Adv. Mater.* **2009**, *21*, 3286–3306.
34. Banerjee, R. Redox outside the Box: Linking Extracellular Redox Remodeling with Intracellular Redox Metabolism. *J. Biol. Chem.* **2012**, *287*, 4397–4402.
35. Griffith, O. W.; Meister, A. Glutathione: Interorgan Translocation, Turnover, and Metabolism. *Proc. Natl. Acad. Sci. U.S.A.* **1979**, *76*, 5606–5610.
36. Jiang, X.; Shen, C.; Rey-Ladino, J.; Yu, H.; Brunham, R. C. Characterization of Murine Dendritic Cell Line JAWS II and Primary Bone Marrow-Derived Dendritic Cells in Chlamydia Muridarum Antigen Presentation and Induction of Protective Immunity. *Infect. Immun.* **2008**, *76*, 2392–2401.
37. Steinman, R. M. The Dendritic Cell System and Its Role in Immunogenicity. *Annu. Rev. Immunol.* **1991**, *9*, 271–296.
38. Yan, Y.; Johnston, A. P. R.; Dodds, S. J.; Kamphuis, M. M. J.; Ferguson, C.; Parton, R. G.; Nice, E. C.; Heath, J. K.; Caruso, F. Uptake and Intracellular Fate of Disulfide-Bonded Polymer Hydrogel Capsules for Doxorubicin Delivery to Colorectal Cancer Cells. *ACS Nano* **2010**, *4*, 2928–2936.
39. Sexton, A.; Whitney, P. G.; Chong, S.-F.; Zelikin, A. N.; Johnston, A. P. R.; De Rose, R.; Brooks, A. G.; Caruso, F.; Kent, S. J. A Protective Vaccine Delivery System for *in Vivo* T Cell Stimulation Using Nanoengineered Polymer Hydrogel Capsules. *ACS Nano* **2009**, *3*, 3391–3400.